Agricultural and Forest Meteorology 228–229 (2016) 265–275

Contents lists available at ScienceDirect

Agricultural and Forest Meteorology

journal homepage: www.elsevier.com/locate/agrformet

Crop lodging induced by wind and rain

P. Martinez-Vazquez

School of Engineering, University of Birmingham, B15 2TT, UK

ARTICLE INFO

Article history:
Received 28 April 2016
Accepted 1 July 2016
Available online 25 July 2016

Keywords:
Crop lodging
Wind simulation
Environmental modelling
UKCP09 weather generator

ABSTRACT

A methodology to estimate wind and rain effects on the four main growth crops in the United Kingdom is presented. The method is based on simulated weather scenarios acting on synthetic plants over a period of thirty years. The environmental data is generated with the UKCP09 Weather Generator considering future climate scenarios whereas plants are modelled as simple oscillators characterised by their mass, stiffness and damping. The joint probability of occurrence of wind and rain are estimated together with the conditions in which lodging would occur. The paper shows that the dynamic response of plants varies with season being the first three months of the year the most critical whilst the plants' performances define crop failure velocities ranging between 4 ms^{-1} and 23 ms^{-1} and associated failure rates of 50% and 5% per unitary velocity.

1. Introduction

The interaction of plants with the wind and the nature of plant failures which can occur during periods of high winds have been much investigated in the past. In Wright (1965) it was noticed that the characteristics of the flow through a canopy varied within the crop height and hence some parameterisation of the observed variation was proposed. Baines (1972), Denmead and Bradley (1967), Finnigan and Mulheran (1978), and Cionoco (1972) also discussed the nature of turbulence within canopies and provided additional insight of the flow dynamics that govern the energy flow exchange in canopies. A review of the interaction of plants with the wind can also be found in de Langre (2008). In terms of plant's modelling, Sellier et al. (2006) investigate the oscillation of trees via numerical modelling whilst Rodriguez et al. (2009) carried out experimental work to determine natural frequencies of walnut trees. For isolated plants the work of Baker (Baker, 1995; Baker et al., 1998; Sterling et al., 2003; Berry et al., 2003; Saunderson et al., 1999, 2000) is notable. Baker (1995) assumed that wheat plants and isolated trees could be idealised as two simple masses connected by a light inextensible element. The first mass represented the root-soil structure of the plant while the second represented the mass of the plant. Baker's model enabled the maximum wind induced base bending moment to be obtained which seemed reasonable when compared to the natural variations which can occur in the plant properties (e.g. stem diameter, root plate spread etc.). More recently, Martinez-Vazquez and Sterling (2011) showed that the model proposed in Baker (1995) can in fact be used to calculate lodging for large populations of plants. The present investigation builds on previous research and attempts to merge mechanical modelling techniques for plants with statistical predictions of environmental variables to calculate crop's behaviour. Environmental variables are simulated by the UKCP09 Weather Generator. This is a virtual facility that enables constructing future climate scenarios from where rain and wind conditions can be determined. In this investigation wind and rain scenarios are used to test plant crops in order to observe conditions that induce their failure. Four types of plants are considered, these are oats, wheat, barley, and rapeseed. The similarities and differences amongst the various plant responses are compared and discussed throughout.

The paper is organised as follows. Section 2 outlines the characteristics of the weather generator and its prediction capabilities; Section 3 provides the details of how to generate wind and rain databases based on the prediction tool; Section 4 describes how the wind turbulence within a canopy was modelled; Section 5 details the generation of synthetic plants, taking oats as a case study; Section 6 explains how to estimate the plant's resistance for the use of Baker's simplified model; Section 7 give full results of the response of oat crops subject to wind and rain; Section 8 extends the plant response analysis to the other plant types, whilst Section 9 provides some final remarks.

2. The UKCP09 weather generator

In recent years the Met Office Hadley Centre in collaboration with UK Climate impacts Programme and over thirty other organisations have developed the UKCP09 Weather Generator aiming at

E-mail address: p.vazquez@bham.ac.uk

http://dx.doi.org/10.1016/j.agrformet.2016.07.003
0168-1923/

Table 1
Peak values of environmental parameters (q_{param}) related to the reference evapotranspiration.

T (°C)	e_d kPa	e_a kPa	R_n MJm^{-2}day^{-1}	U_2 (ms^{-1}) Eq. (2)	U_2 (ms^{-1}) Full-scale
18.04	1.52	2.01	11.56	3.85	3.5

visualising future climate fluctuations across the United Kingdom. This facility is capable to provide weather scenarios and associated measures of uncertainty until 2080. In the present research this tool was used to determine the most probable combinations of wind and rain that are likely to occur on the region of Cardington, UK (52.1055°N, 0.4244°W 29 m above MSL) and to evaluate their combined effect on oat crops.

The UKCP09 user's interface provides access to customised outputs that reflect the underlying UKCP09 climate projections. Pre-prepared maps and graphs can be used to select any land or marine region—defined by 5 km^2, within the UK. The available data includes 17 variables over land areas and 4 over marine regions. The following are the weather parameters over land areas that can be generated by using the referred tool (Jenkins et al., 2009).

- Mean temperature (°C)
- Mean daily maximum temperature (°C)
- Mean daily minimum temperature (°C)
- 99th percentile of daily maximum temperature in a season (warmest day of the season) (°C)
- 1st percentile of daily maximum temperature in a season (coolest day of the season) (°C)
- 99th percentile of daily minimum temperature in a season (warmest night of the season) (°C)
- 1st percentile of daily minimum temperature in a season (coldest day of the season) (°C)
- Precipitation rate (mm/day)
- 99th percentile of daily precipitation rate in the season (wettest day of the season) (mm/day)
- Specific humidity (%)
- Relative humidity (%)
- Total cloud (%)
- Net surface long wave flux (W/m^2)
- Net surface short wave flux (W/m^2)
- Total downward short wave flux (W/m^2)
- Mean sea level pressure (hPa)
- Grass reference evapotranspiration (mm/day)

Environmental data for any selected region are accessed by setting up a request to the UKCP09 central unit, for example by following the procedure given in Appendix A. After the request is made the simulated data is made available for the user to download.

3. Hourly rain and wind database

The amount of rain per day and per hour is directly available from the output of the UKCP09 simulator but not for the velocity of the wind. In such case one can estimate the hourly wind regime through a two-step process namely (i) inferring the daily winds by using the grass reference evapotranspiration parameter (only available on a daily basis) and (ii) downscaling the data to estimate hourly winds. The way this process was applied for this research is described in the following paragraphs.

3.1. Daily wind

There are a number of methods to infer the wind from the environmental parameters such as those discussed in Ventura et al. (1999), Allen et al. (1994), Ekström et al. (2007), and Eames et al. (2011), to mention some. These approaches are based on the reference evapotranspiration ET_0 which is calibrated based on full-scale observations. In this research the 24-h FAO Penman-Monteith equation – as described in Ventura et al. (1999), was used. This approximation is given by Eq. (1) below.

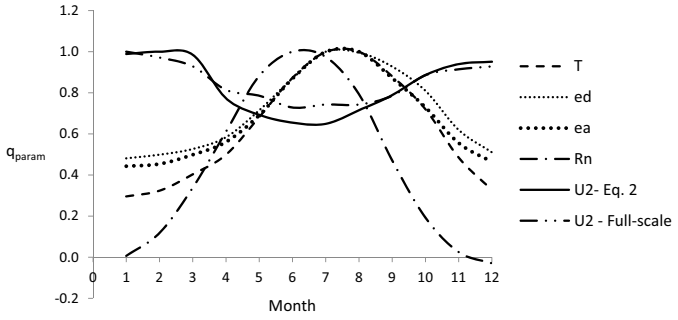

Fig. 1. Monthly average of environmental parameters related to *PET*.

$$PET = \frac{0.408\Delta\,(R_n - G) + \gamma \frac{900}{T+273.16} U_2\,(e_a - e_d)}{\Delta + \gamma\,(1 + 0.34U_2)} \quad (1)$$

1 PET : grass reference evapotranspiration (mm day^{-1})
2 R_n : net radiation at crop surface (MJ m^{-2} day^{-1})
3 G : soil heat flux (MJ m^{-2} day^{-1}) – assumed to be zero as in Ekström et al. (2007)
4 T: mean temperature at 2 m height (°C)
5 U_2 : wind speed measured at 2 m height (m s^{-1})
6 $(e_a$-$e_d)$: vapour pressure deficit for measurement at 2 m height (kPa)
7 Δ : slope of the vapour pressure curve (kPa °C^{-1})
8 γ : psychrometric constant (kPa °C^{-1})
9 900 : coefficient for the reference crop (kJ^{-1} kg K day^{-1}) – see Allen et al. (1994)
10 0.34 : wind coefficient for the reference crop (s m^{-1})

Eq. (1) can be re-arranged as in Eq. (2a) in order to infer daily mean velocities of wind.

$$U_2 = \frac{PET\,(\Delta + \gamma) - X}{(YZ - 0.34\gamma PET)} \quad (2a)$$

where

$$X = 0.408\Delta\,(R_n - G); \quad Y = \gamma \frac{900}{T + 273.16}; \quad Z = e_a - e_d \quad (2b)$$

The equations to calculate all parameters for estimating U_2 in Eq. (2a) are given in Appendix B.

The data provided by the weather generator was passed through Eq. (2) and then averaged per month in order to establish a comparison with full-scale statistics issued by in Met Office (2013) —in terms of wind velocity. The results of the data processing for hundred scenarios of 30-years each are presented in normalised form in Fig. 1 whilst Table 1 provides the peak values of each environmental parameter. Note that full-scale measurements have been normalised by the peak simulated value in order to show the actual relationship between the two vectors.

In Fig. 1 is seen that the net radiation profile (R_n) is out of phase with respect to temperature (T) which might be due to the influenced of solar declination and relative distance with respect to the sun. Actual (e_d) and saturated (e_a) vapour pressure seem strongly correlated to T whilst the peak wind velocity occurs near the equinoxes, which is consistent with full-scale observations.

Table 2
Peak and average values of U_2 as inferred from Met Office (2013).

Month	1	2	3	4	5	6	7	8	9	10	11	12
$U_{2,peak}$	15.2	15	14	12.4	12	11.3	11	11.2	12	12.5	13.7	14.5
$U_{2,mean}$	7	6.8	6.5	5.7	5.5	5.1	5.2	5.2	5.2	6.2	6.5	6.5

The average ratio full-scale to simulated wind data is of 1.045. Thus according to the UKCP09 future scenarios, wind velocity will increase or decrease at a rate of about 4.5% within a horizon of 30 years (Jenkins et al., 2009).

Full-scale data was inferred from the Virtual Met Mast Report (Met Office, 2013) which is located in Cardington, UK. For that report measurements were taken at a height of 50 m thus for the purpose of comparison the data was scaled to 2 m above the ground by using the relationship $U_z = (z/z_r)^{\Upsilon}$ with $z_r = 10$ m and $\Upsilon = 0.22$. The inferred average and peak reference values used here are provided in Table 2.

3.2. Hourly wind

The average hourly winds registered at Cardington (Met office, 2013) exhibit day fluctuations that can be approximated by Eq. (3)—where $\hat{U}$ represents hourly velocity normalised by the mean value. U_{24} and t, are the velocity at 24-h and time of the day (hr) respectively.

$$\hat{U} = A\left[-sin\left(\frac{\pi(t-F)}{Fx}\right)\right] + \frac{t(t-E)}{BC} + D \cdot U_{24} \quad (3)$$

with $A = 0.16$; $B = 60$; $C = 22$; $D = 1.13$; $E = 31$; $F = 22$; $x = 0.63$

The estimated mean square error between the proposed Eq. (3) and full-scale measurements was of about 1.11%. This approximation was used to infer hourly winds from daily records followed by monthly probability distributions. The latter are shown in Fig. 2a whereas Fig. 2b shows average probability distributions calculated per period of three months. Similarly future scenarios provided by the UKCP09 Weather Generator were used to calculate the probability distribution of daily rain which is shown in Fig. 3.

In Fig. 2a the change of maximum wind speed over the year has been reflected. The wind velocity tends to be lower during summer and therefore their probability distribution P $[q \leq U_2]$—where q is the instantaneous velocity at 2 m above the ground, exhibits higher rates of change in comparison with winter times. This can be more clearly appreciated in Fig. 2b where three-month averages have been represented. In the case of rain the records show an increase towards the end of the year with less variation during the first six months. Three-month averages suggest that the amount of daily rain is fairly uniform during the year. However note that the probability distribution shown in Fig. 3 does not reflect the probability of precipitation but the level of rain when it does occur. The former i.e. P $[i > 0]$, was estimated separately and is provided in Table 3. Fig. 3 also predicts that within a horizon of 30 years the amount of rain that will be exceeded 50% of the time ranges between 1.75 mm (Apr) and 2.75 mm (Nov) which is consistent with the expected value of 2 mm that has characterised the UK – see Baker et al. (1998).

The probabilistic analysis was completed by defining Weibull distribution curves to characterise hourly winds and accumulated rain per month. Eq. (4) gives the general form of the Weibull function whilst Table 3 shows the shape (ϑ) and scale parameters (α) that resulted from the analysis. Note that the variable x in Eq. (4) represents wind or rain.

$$(v) = \frac{\vartheta}{\alpha}\left(\frac{x}{\alpha}\right)^{\vartheta-1} e^{-\left(x/\alpha\right)^{\vartheta}} \quad (4)$$

Table 3
Weibull parameters that represent probability density functions for wind and rain.

Month	Wind (U_2)		Rain (i)		P[$i > 0$]
	ϑ	α	ϑ	α	
1	2.2	4.8	0.76	2.6	0.497
2	2.2	4.8	0.76	2.4	0.439
3	2.1	4.7	0.76	2.4	0.451
4	1.82	3.8	0.80	2.0	0.472
5	1.53	3.3	0.85	1.8	0.388
6	1.67	3.3	0.70	2.9	0.335
7	1.74	3.3	0.70	2.6	0.347
8	1.95	3.8	0.75	3.1	0.314
9	2.0	4.0	0.75	2.8	0.378
10	2.0	4.1	0.75	3.4	0.379
11	2.3	4.6	0.80	3.9	0.459
12	2.0	4.6	0.75	3.3	0.460

The value of shape factors shown in Table 3 indicate that rain is a highly skewed process resembling an exponential form whilst hourly wind is asymmetric with respect to the mean value. The average shape factor predicted by the UKCP09 Weather generator across the year is of 1.96. The Met Office (2013) reports a shape factor of 2.16 for historical data referred to 50 m above the ground level. However these measurements correspond to different heights the increase of skewness of pdfs as the locations approaches to the ground seems reasonable.

Finally, Fig. 4 shows an overview of the variability of hourly wind and accumulated rain over the year in normalised form. In this figure the peak value of wind is of 3.85 as indicated in Table 1, whereas the peak value of accumulated rain during the month is of 54.4 mm.

4. Wind turbulence within the canopy

Finnigan (2000) has shown that turbulence within plant canopies differs from that of the surface layer. This variation is due energy short-cutting of the spectral cascade due to vortex shedding on the plants (larger eddies broken up into smaller eddies very rapidly). Thus the energy loss that occurs inside the canopy should be considered when estimating wind effects on cereal crops. Finnigan (2000) presents the variation of the spectral density $nS_u(n)/\sigma^2$ with $n\phi$ where $\phi = h_c/U(h_C)$—being $U(h_C)$ and h_c the average mean velocity inside the canopy and the height of the crop respectively. Although no equation to generate the continuous spectral density is provided by Finnigan (2000) it has been observed in this study that the shape of the spectrum is similar inside and outside the canopy. This is demonstrated in Fig. 5 which compares a scaled version of the Von Karman's wind power spectrum—given by Eq. (5), with the results presented by Finnigan (2000). In Eq. (5) the reduced frequency $n\phi$ is taken as independent variable as in Finnigan (2000). It follows that a suitable scaled version of the standards wind power spectrum can be used to represent turbulence inside the canopy. The recommended spectrum to represent turbulence inside the canopy is thus given by Eq. (5).

$$\frac{nS_u(n)}{\sigma^2} = \frac{4(n\phi)}{\left(1 + 70.8(n\phi)^2\right)^{5/6}} \quad (5)$$

The estimated mean square error between Eq. (5) and the spectrum presented by Finnigan (2000) is of 6.6% whereas in the region $0.1 \leq n\phi \leq 100$ one obtains a mean square error of about 0.09%. The

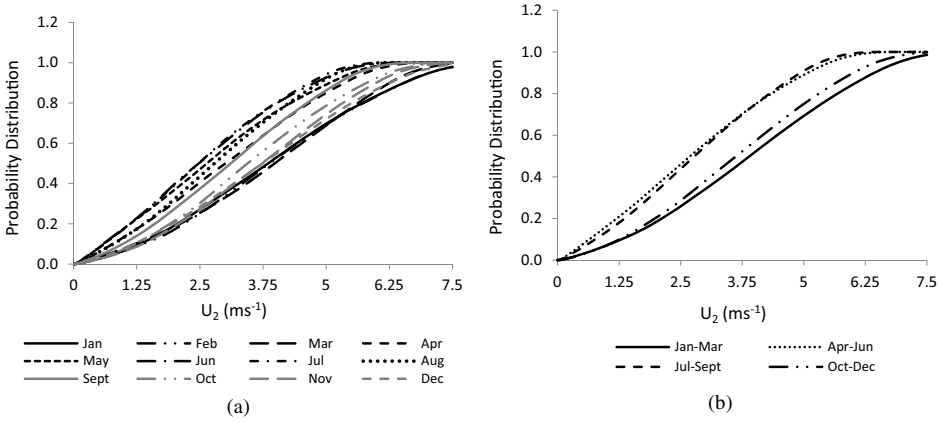

Fig. 2. Probability distribution for wind (a) per month and (b) three-month average.

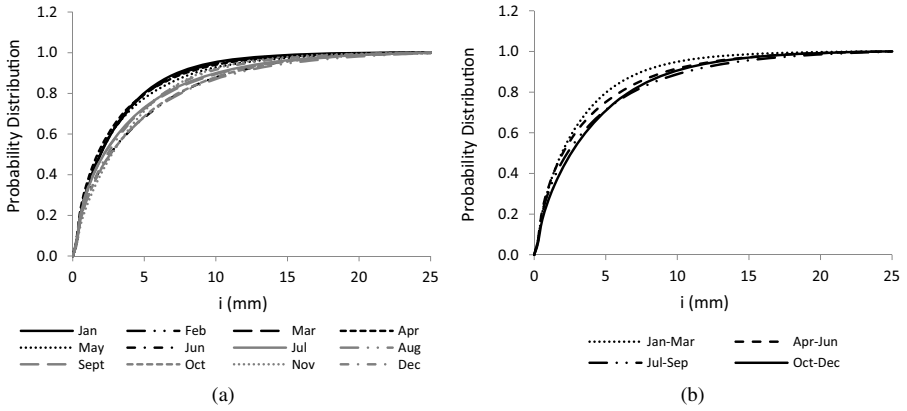

Fig. 3. Probability distribution for rain (a) per month and (b) three-month average.

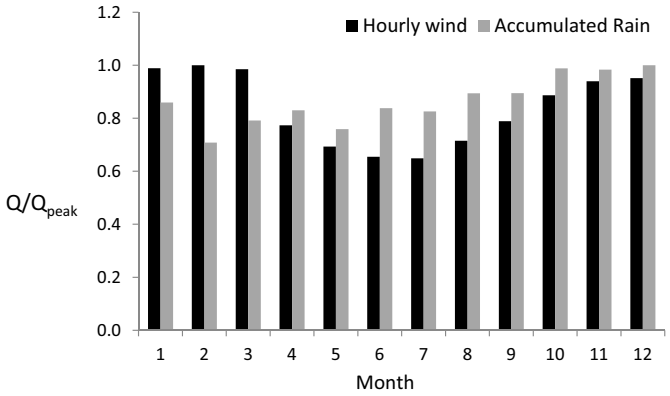

Fig. 4. Variation of hourly wind and accumulated rain across a year (30-year horizon).

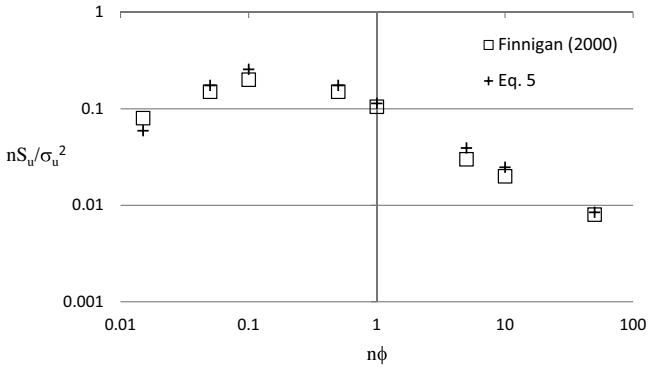

Fig. 5. Spectral representation of turbulence inside plant canopies.

relevance of the spectral region above 0.1 Hz is that it covers any natural period of a cereal plant that is below 10 s which is presumably 100% of the crop. Based on this results it has been decided to use Eq. (5) to represent wind turbulence within plant canopies.

5. Plant database

Berry et al. (2003) have parameterised wheat plants by using data collected across 32 crops in the UK. In that study partial correlation amongst some of the plant parameters have also been established. The parameters used by Berry et al. (2003) to characterised wheat are:

- Centre of gravity (X) : mm
- Ear area (A): mm^2
- Stem diameter (d) : mm
- Natural frequency (n) : Hz
- Root plant depth (h) : mm
- Root plant spread (D) : mm
- Stem wall width (t) : mm
- Material strength (R) : Nmm^{-2}
- Shoot number per plant (N)

whereas partial correlation found amongst some of the parameters are as in Eq. (6),

$$t = 0.22d + 0.097 \quad (6a)$$

Table 4
Parameters used to characterise oat plants.

	X	A	d	n	h	D	t	R	N
mean	950	10000	6.6	1.4	70	50	1.0	30	2.5
stdev	150	3000	1.0	0.2	10	10	0.2	5	0.5

$$D = 5.46N + 20.5 \tag{6b}$$

$$n = X^{-3/2} + 0.3 \tag{6c}$$

In the following paragraphs a similar approximation is used to characterise oats. Later on the simulation method will be extended to three other types of plant. In line with that, oats can be characterised by using the values listed in Table 4. These are average values derived from one or more varieties of the oat cereal as discussed by Berry et al. (2013) and Baker et al. (2014).

A 20-plant database was initially generated in order to tests oats to subject to different levels of wind and rain. In generating the database all the parameters listed in Table 4 have been considered to be normally distributed and, with exception of *t*, *D*, *X*, *d*, *n*, *and N*, uncorrelated—see Eq. (6). The procedure followed to run the plant's simulation basically consists of generating a series of random numbers to be projected on the cumulative distribution function of uncorrelated plant parameters to find values of the plant parameters. The plant database generated in this way is presented in Table 5.

6. Plant resistance

Plant failure can occur by root or stem insufficient resistance. The former is a function of soil moisture and extent of the root whereas the latter depends on mechanical properties and geometry of the stem. Baker et al. (1998) provides the equations that allow the bending capacity of the root (M_r) and stem (M_s) to be estimated. For the benefit of the reader those equations are reproduced here in Eqs. (7) and (8).

$$s_w = 1484e^{-5f/c}(2.2 - 0.24\nu)(4.82c - 0.30) \tag{7a}$$

$$s_d = 1125e^{-5w/c}(2.2 - 0.24\nu)(4.82c - 0.30) \tag{7b}$$

$$s = s_d - \frac{i}{\rho_s/\rho_w (f - w)h}(s_d - s_w) \geq s_w \tag{7c}$$

$$M_r = k_s s D^3 \tag{7d}$$

Table 6
Soil parameters.

k_s	*i*	*c*	*v*	*w*	*f*
0.43	2.0	0.25	5	0.15	0.27

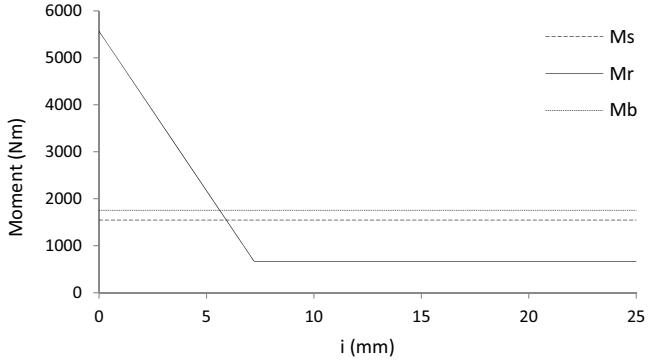

Fig. 6. Typical relationship between stem and root resistance with wind-induced bending acting – oat plant 13.

The stem failure moment is given by,

$$M_s = \frac{\sigma\pi d^3}{32}\left(1 - \left(\frac{d/2 - t}{d/2}\right)^4\right) \tag{8}$$

In these equations s_w, s_d are the shear strength for wet and dry soil conditions respectively, ρ_s and, ρ_w represent soil and water density, *i* is the daily rainfall that is exceeded 50% of the time, *c* is the clay content, *v* is a visual score measuring soil compaction, *w* is the water content at wilting point and *f* represents the water content at field capacity. The values for these parameters used in this study are provided in Table 6.

Based on Eq. (7)–(8), and using the parameters listed in Tables 5 and 6 a typical relationship between M_r, M_s, and the bending moment induced by wind (M_b) could be defined. Note that M_b is simply the result of multiplying the wind force $F_w = 1/2\rho_{air}C_D U_2^2 A$ by the corresponding distance *X*—where C_D and *A* are the drag coefficient and area exposed to wind respectively—see Table 5. Fig. 6 shows values of M_s, M_r and M_b calculated for plant 13 and for different levels of rain (*i*).

Table 5
20-Plant database.

Plant	X	A	d	n	h	D	t	R	N
1	789.33	5015.79	6.44	1.5	66.34	54.86	1.24	33.36	2.18
2	973.68	4891.84	7.87	1.24	95.4	43.69	0.39	24.82	2.78
3	1150.08	4523.18	5.94	1.21	59.38	43.95	0.92	30.8	2.28
4	988.83	4838.33	6.11	1.7	49.19	57.55	1.12	29.79	2.4
5	1131.78	5031.35	5.79	1.64	46.12	39.72	1.19	27.71	2.59
6	790.23	4561.14	5.96	1.73	67.69	45.65	1.07	25.69	2.28
7	979.68	5232.15	6	1.71	75.23	46.76	1	23.88	2.6
8	1110.18	4524.55	6.73	1.19	49.79	65.22	1.2	29.99	1.98
9	920.28	5412.38	7.69	1.45	70.77	52.6	1.01	22.14	2.95
10	964.53	3737.81	7.08	1.44	70.79	59.78	0.79	36.69	1.75
11	973.68	4857.08	7.35	1.19	61.07	53.06	0.78	33.3	2.32
12	892.83	4055.72	7.92	1.72	75.06	42.78	0.86	26.84	2.97
13	903.03	4965.48	7.83	1.21	50.13	63.44	1.07	32.83	1.82
14	801.94	4642.1	5.41	1.58	55.25	50.4	1.04	28.41	2.51
15	848.58	4700.65	6.4	1.4	68.19	58.8	0.86	30.93	2.69
16	1027.68	5035.46	4.46	1.59	74.88	51.39	0.98	22.11	2.41
17	953.88	4030.1	5.66	1.35	72.59	61.59	0.89	20.23	2.08
18	1116.93	4648.96	6.11	1.32	70.69	40.4	0.8	30.89	2.95
19	756.33	4371.78	5.84	1.47	72.47	46.95	0.89	22.87	2.88
20	896.28	4770.63	6.78	1.33	74.52	60.99	1.02	22.82	3.24
mean	948.49	4692.32	6.47	1.45	66.28	51.98	0.96	27.81	2.48
stdev	118.46	413.73	0.93	0.19	11.96	8.03	0.19	4.61	0.41

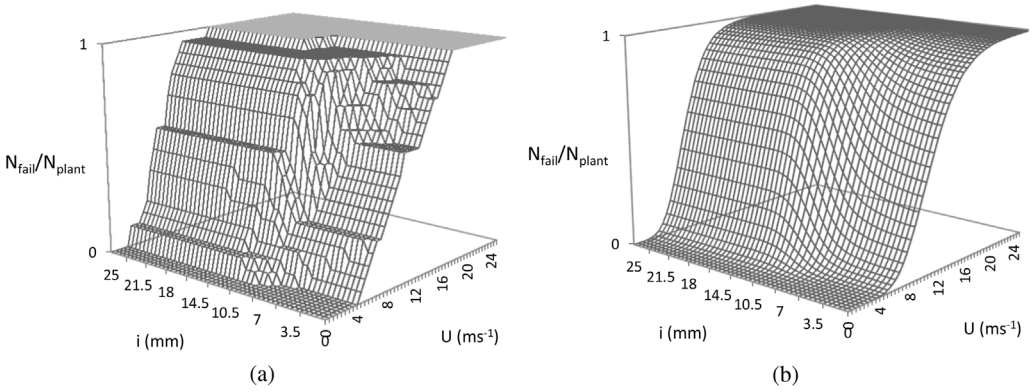

Fig. 7. Representation of Failure for the oat crop based on (a) 20-plant database and (b) 10 000 plant sample.

In Fig. 6 two regions that characterise crop failure can be identified. The first one controlled by stem resistance which according to the simulated database covers the lower precipitation range i.e. $0 \le i < 5$-10 (mm) whereas the second region of failure corresponds to precipitation rates above 5–10 (mm) leading to root failure. According to Eq. (7c) the root capacity is bounded by the soil shear strength at wet condition. This is consistent with Baker et al. (1998) where Eq. (7c) is validated for the interval $0 \le i \le h\ (f-w)\rho_s/\rho_w$ which for the average soil parameters and plant characteristics presented above translate into an upper limit of ~7.15 mm. In the following the lower shear strength of the soil will be considered to be constant across high rain conditions i.e. $h(f-w)\ \rho_s/\rho_w \le i \le 25$ mm in order to observe the crop behaviour under high winds however keeping in mind the identified boundary conditions.

7. Analysis of plant's response

The force induced to the plants by wind were estimated and their demand of resistance was compared against the capacity to resist the overturning moments provided by the root and the stem. This was done for a range of wind and rain levels so that the number of plants that failed could be quantified. Fig. 7a shows the quantification of failure in terms of the index N_{fail}/N_{plant} for the 20-plant database presented in Table 5—where N_{fail} and N_{plant} are number of failed plants and number of plants in the original database respectively. Fig. 7b shows the quantification of failure for an extended database including 10 000 plants. Note that the extended database was formed by using the methodology described in Section 5 for the 20-plant sample.

In Fig. 7 the two regions of failure identified in Fig. 6 have been reflected. The first region being determined by stem failure occurring for rain levels of $0 \le i \le h(f-w)\ \rho_s/\rho_w$ and characterised by a constant value of the index N_{fail}/N_{plant} with respect to i—more clearly appreciated on Fig. 7a where $h(f-w)\rho_s/\rho_w$ fluctuates around 7.15 mm. For levels of rain that exceed $i = h(f-w)\rho_s/\rho_w$ there is a bi-linear type of behaviour as i varies, which is predicted by Eq. (7) and (8) and illustrated in Fig. 6.

In order to better visualise the lodging for the domain $\{U, i\}$ presented in Fig. 7b, a range of curves representing plant failure for various levels of i are represented in Fig. 8.

The shape of the curves in Fig. 8 is consistent with the Weibull distribution function for wind velocity (U) whose parameters are given in Table 3. It can be seen in this figure that the rate of failure increases with the level of rain. However note that no significant variation was observed for levels of rain above 12 mm—which can also be seen in Fig. 7b, and therefore the curve shown in Fig. 8 for $i = 12$ mm can be considered constant for higher levels of rain.

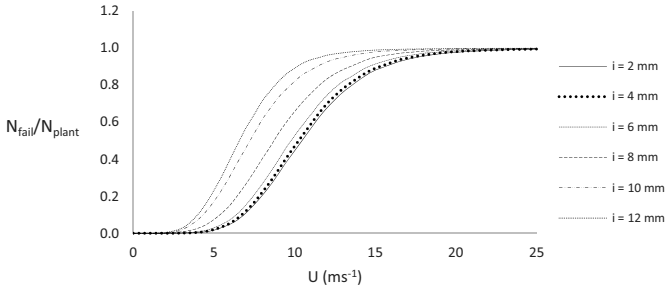

Fig. 8. Index of Failure for the 10 000 plant sample for different levels of rain.

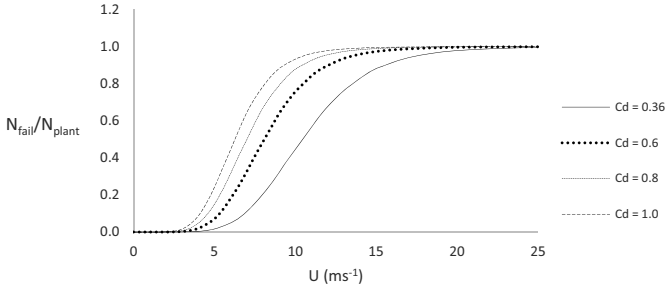

Fig. 9. Index of Failure for the 10 000 plant sample for $i = 2$ mm and different values of Cd.

On the other hand, given the limited amount of experimental work undertaken as to determine the drag coefficient on oat plants (Verissimo, 2015), a parametric analysis was undertaken to investigate the percentage of plants' failure for different values of Cd and for a rain level of 2 mm. The results of this is shown in Fig. 9 for values of Cd equal to 0.36, 0.6, 0.8, and 1.0. Note that the results shown in Figs. 6–8 were estimated by considering Cd of 0.36 i.e. the lower value in the range.

Fig. 9 shows that the increase of lodging is not linear with the variation of Cd. This might be due to the fact that as the plant takes more load the mode of failure can switch from stem to root failure and vice versa depending on the characteristics of the root. Note for instance that whereas about 95% of the crop would have failed for when Cd equals 1.0 and U reaches 10 ms^{-1} only about half of it would have done so when Cd equals 0.36 and for the same level of wind.

Finally, the probabilistic description for wind and rain at the locality of Cardington, given in Section 3 was used to determine the probability associated to oat failure whilst subject to the combined effect of wind and rain. Since wind and rain are considered to be

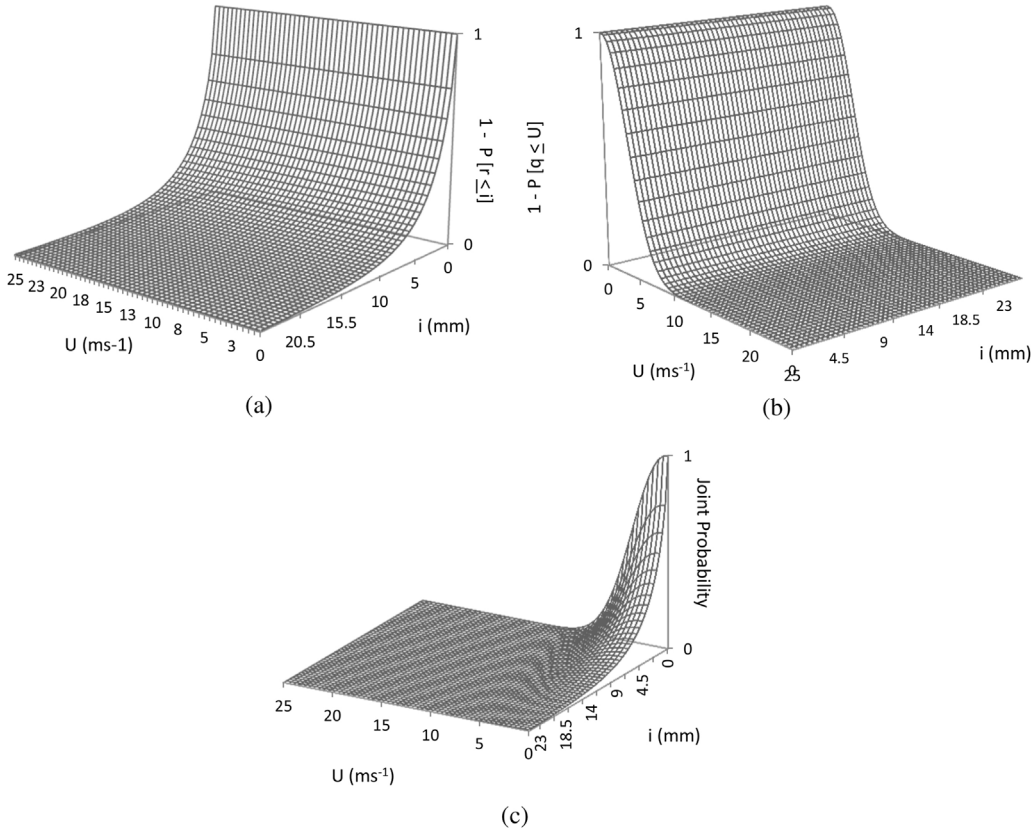

Fig. 10. Probability of i and U being exceeded (a, b) together with their joint probability (c).

Table 7
Probability of failure of oat crop (%) for $i = 2$ mm.

U (ms^{-1})	Rain Season			
	Jan	Apr	Jul	Oct
2	0.0	0.0	0.0	0.0
4	0.08	0.04	0.04	0.07
6	0.42	0.18	0.13	0.3
8	0.42	0.16	0.08	0.23
10	0.13	0.05	0.02	0.06
12	0.02	0.01	0.0	0.01
14	0.0	0.0	0.0	0.0
16	0.0	0.0	0.0	0.0
18	0.0	0.0	0.0	0.0
20	0.0	0.0	0.0	0.0

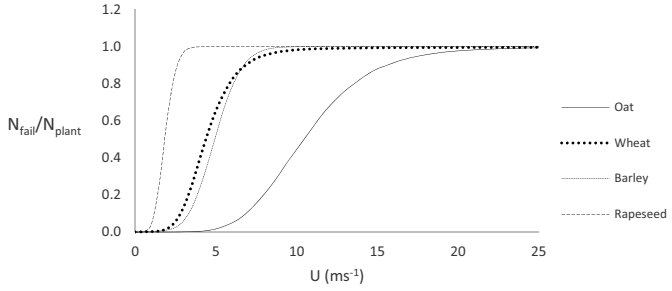

Fig. 11. Representation of plant's failure when $i = 2$ mm.

uncorrelated[1] the probability of plant failure associated to each pair $\{U, i\}$ is taken as the product of the probability associated to U_j and i_k being exceeded, times the index N_{fail}/N_{plant}—see Eq. (9).

$$P[M_b > M_s || M_b \rangle M_r] = (1 - P[r \leq i]) \cdot (1 - P[q \leq U]) \cdot \frac{N_{fail}}{N_{plant}} \qquad (9)$$

where r, q are random variables representing rain and wind respectively. A description of the probability that daily rain and hourly wind are exceeded together with the corresponding joint probability are given in Fig. 10. The estimated probability of failure—see Eq. (9), for a range of wind speeds occurring for daily rain of 2 mm is shown in Table 7.

It can be seen in Fig. 10c that the combined action of i and U makes the crop failure more suceptible to occur at relatively low levels of rain and wind. This is because the curves shown in Fig. 10 are fairly flat at high values of i and U. Moreover, the region of higher joint probability of the pair $\{i, U\}$ being exceeded coincides with low frequency of failure shown in Fig. 7b. This translates into low probability of failure for the oat crop as shown in Table 7 for a selected number of seasons and for $i = 2$ mm.

In Table 7 can be seen that the probability of failure varies with i and it tends to be higher early or late during the year i.e. whilst wind loads tend to increase as shown in Fig. 4. Moreover through a more general analysis it was observed that the highest probability of failure during January was estimated as of 0.81%, occurring around the pair $\{i = 0.5\ mm, U = 7\ ms^{-1}\}$. This suggests that oat crops would have a rather low probabilty of failure in any season. In the following section it is shown that wind can have an important impact on lodging associated to other types of plants.

[1] This is an assumption and is also the assumption in Baker et al. (2014). Although it can be argued that some correlation exists for stronger winds (Tsimplis, 1994), there is not enough evidence to assume there is correlation at medium or low wind levels.

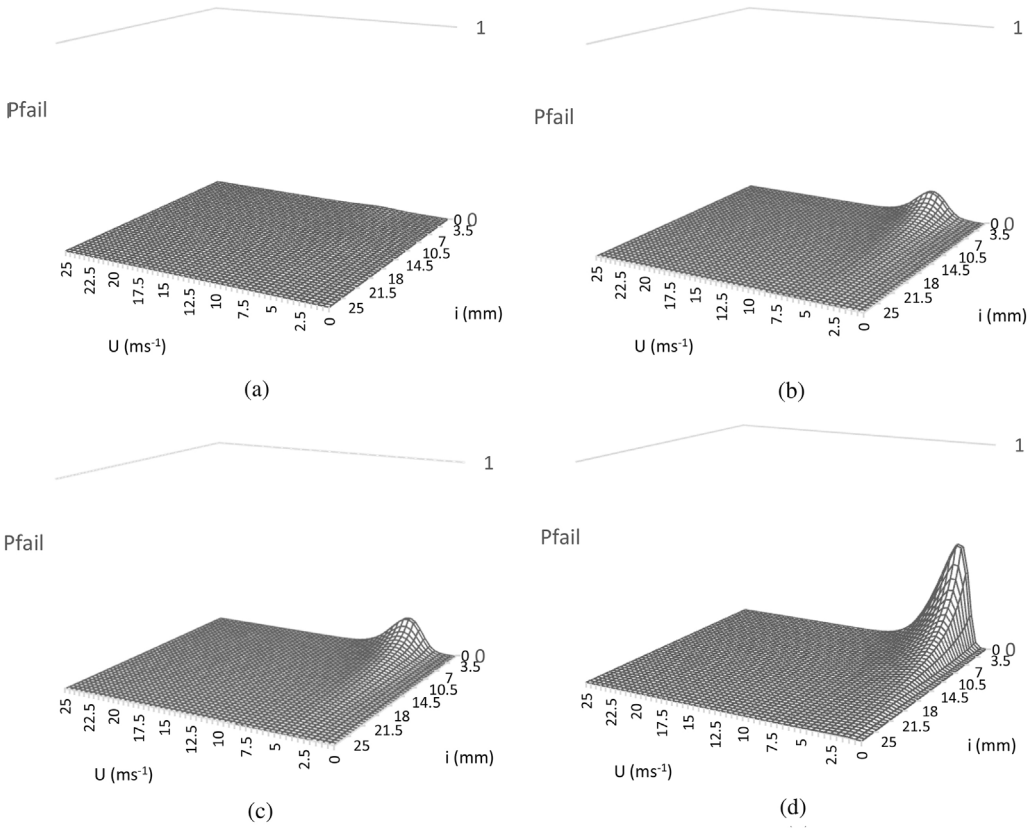

Fig. 12. Probability of failure of (a) oat, (b) barley, (c) wheat, and (d) rapeseed, during January.

8. Crop failure characterising four types of plants

The analyses above were extended to three other plant types. These are wheat, barley, and oilseed rape i.e. those which together with oat are reported as the most produced in the UK (Verissimo, 2015). The parameters that characterise these cereal plants are provided in Table 8. Note that the parameter k_s refers to the root resistance defined by Eq. (7d) whilst m represents the characteristic mass of the plant's ear. For the sake of clarity, the oat parameters presented in Table 4 have also been included in Table 8.

In line with the analysis described above, plant databases conformed by 10,000 elements were subject to the combined action of wind and rain. Fig. 11 shows the estimation of plant failure in terms of the index N_{fail}/N_{plant}, for all the groups. For the sake of simplicity only those results calculated for 2 mm of rain are shown.

In Fig. 11 can be seen that rapeseed is the more susceptible to fail, opposite to oat which could withstand wind speeds of 10 ms^{-1} and above. Wheat and barley have a similar behaviour with slight differences below and above a wind speed of around 6.5 ms^{-1}–the point where their performance seems to match. The results obtained also enable an average failure velocity to be inferred. Let that threshold value be the velocity of wind at which ~50% of the crop fail. According to this the mean failure velocity for the plant types analysed is of approximately 1.6 ms^{-1}, 4.5 ms^{-1}, 5 ms^{-1}, and 10.5 ms^{-1}, for rapeseed, wheat, barley, and oat, respectively. Similarly the ultimate failure velocity i.e. the one that would virtually cause total failure of the crop, is of 4.0 ms^{-1}, 8.5 ms^{-1}, 12 ms^{-1}, and 23 ms^{-1} for rapeseed, barley, wheat, and oat, respectively. Note that these reference velocities are valid for a level of rain of 2 mm.

On the other hand, based on Eq. (9), the probability of plant's failure was calculated. As noted above the shape of the joint prob-

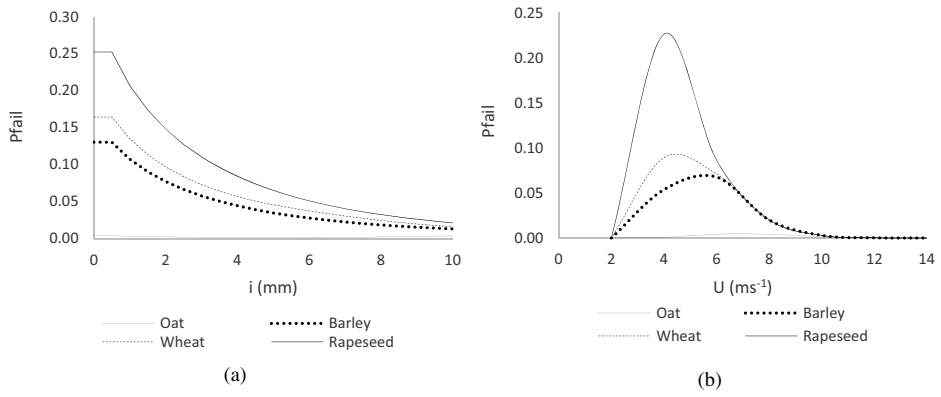

Fig. 13. Probability of failure estimated for all plant types (a) with $U = 5$ ms^{-1} and (b) with $i = 2$ mm.

Table 8
Parameters used to characterise target plant types.

Plant Parameter	Plant Type–Mean Value				Plant Type–Standard Deviation			
	Oat[a]	Wheat[b]	Barley[c]	Rapeseed[a]	Oat[a]	Wheat[b]	Barley[c]	Rapeseed[a]
X (mm)	950	426	800	1520	150	34.08	65	200
A (mm^{-2})	10000	8000	9500	37000	3000	800	280	3000
d (mm)	6.6	3.35	5.32	11.1	1.0	0.402	0.85	2.0
n (Hz)	1.4	0.92	0.75	0.5	0.2	0.138	0.093	0.1
h (mm)	70	40	90	123	10	8.0	12.5	15
D (mm)	50	38	44	16.5	10	8.36	12.75	3.0
t (mm)	1.0	0.64	1.35	2.2	0.2	0.147	0.16	0.5
R (Nmm^{-2})	30	30	27	25	5.0	9.9	2.8	5.5
m (Kg)	0.008[c]	0.006[c]	0.005	0.01[d]	–	–	–	–
k_s	0.43	0.43	0.58[e]	4.0[a]	–	–	–	–
N	2.5	3.2	4.4	8.2	0.5	1.152	0.5	1.0

[a] Baker et al. (2014).
[b] Berry et al. (2003).
[c] Verissimo (2015).
[d] Author's estimate based on Berry et al. (2013).
[e] Berry et al. (2006).

ability distribution restricts the lodging domain in the direction of both variables i and U. This can be observed in Fig. 12 which corresponds to the first month of the year – the season identified as critical for lodging to occur.

The results presented in Fig. 12 confirm the low susceptibility of oat crops to fail. As discussed in the previous section the highest probability associated to oat lodging is of 0.81%. The peak values observed in Fig. 12 occur at low levels of rain – where according to Eq. (7c) and Fig. 6 lodging would be controlled by stem resistance. Peak values in the curves shown in Fig. 12 are of 0.81% for oat when $U = 7\,ms^{-1}$, 13% for barley with $U = 5.5\,ms^{-1}$, 17% for wheat with $U = 4.5\,ms^{-1}$, and 50% for rapeseed when $U = 3\,ms^{-1}$.

For the sake of clarity the probability of failure derived from crop performances is illustrated in Fig. 13 by using reference values of (a) velocity $U = 5\,ms^{-1}$ and (b) rain $i = 2$ mm.

In Section 6 it was discussed how the plant's root strength increases as i decreases. This is also being reflected in Fig. 13a where is shown that in region of low rain the probability of lodging to occur is being controlled by stem resistance – see also Fig. 6. Fig. 13a also shows that at least for $U = 5\,ms^{-1}$, wheat has more chances to fail than barley whilst both plant types would report ~50% less failure than rapeseed but more than 100% of the failure that can be associated to oat. In Fig. 13b becomes evident that each plant type responds differently when subject to the same level of rain. This is illustrated by the relative position of the peak probability of failure. This figure also shows that the interval $2 \leq U \leq 10\,ms^{-1}$ is where lodging of any crop is susceptible (in a probabilistically sense) to occur. This is in principle valid for a level of rain of 2 mm, however looking at Fig. 12 it seems that no much difference would make to have levels of rain of up to about 10 mm.

9. Final remarks

The paper has shown a method to estimate crop failure by using statistical descriptions of the climate such as those provided by the UKCP09 Weather Generator together an existing theoretical model to calculate the plant's response. The weather scenarios studied cover a horizon of 30 years. The data predicts an increase of wind velocities of about 4.5% with respect to current conditions. The weather predictions also suggest that the level of rain that is exceeded 50% of the time will range between 1.75 mm during April and 2.75 mm in November. That makes a yearly average of 2.25 mm i.e. slightly above the current reference value of 2 mm. Regarding the crop responses, the study identifies oats as the most resilient type of plant from the group whilst rapeseed appears to be the most susceptible to fail. For example the failure velocity for 100% of the oat crop is estimated as of $23\,ms^{-1}$ and it is of $4\,ms^{-1}$ for rapeseed, for a level of rain that is exceeded 50% of the time. The prediction model also indicates that the failure velocity will become constant after a threshold value of rain (that is exceeded 50% of the time) in the region of 7.5 mm i.e. stem failure would dominate the plant's failure after that point. Finally, the proposed research methodology suggests three areas of development: (a) the interaction of plants in motion and with the changes caused in the boundary layer during that process, (b) the availability correlated wind and rain statistics, and (c) development of finite element models that enable to observe the flow of stress and rate of deformation experienced by different segments of plants at the time that allow quantifying lodging i.e. modelling large populations of plants at high resolution.

Appendix A. : Steps to generate climate scenarios by using the UKCP09 Weather Generator

1 Pathway
- i. UK probabilistic projections of climate change over land
- ii. UK probabilistic projections of climate change over marine regions
- iii. Weather generator simulator
- iv. Past and future multi-level ocean simulations for UK waters
- v. Projections of trend in storm surge for UK waters
- vi. Projections of sea level rise for UK waters

Option (iii)

2 Emission scenario
- i. Low
- ii. Medium
- iii. High

Option (ii)

3 Time period
- i. 2020s: 2010-2039
- ii. 2030s: 2020-2049
- iii. 2040s: 2030-2059
- iv. 2050s: 2040-2069
- v. 2060s: 2050-2079
- vi. 2070s: 2060-2089
- vii. 2080s: 2070-2099

Option (i)

4 Location

e.g. Rosemaud, Cardington (52.11 °N, 0.424 °W 83 m above MSL)

5 Sampling method
- i. All
- ii. Random sampling of model variants
- iii. Specific set of model variants
- iv. Particular sub-set of probabilities

Option (ii)

6 Configuring weather generator
- i. Daily
- ii. Hourly

Option (all)

7 Format output file
- i. Map
- ii. Raw data
- iii. Joint probability plot
- iv. Plume plot
- v. Return periods plot
- vi. Cumulative distribution function
- vii. Probability density function

Option (ii) CSV file

Appendix B. : Equations to calculate U_2 from known environmental parameters

$$X = 0.408\Delta\,(R_n - G) \quad \mathrm{Y} = \gamma\frac{900}{T+273.16}; \quad \mathrm{Z} = e_a - e_d \tag{B1}$$

$$\Delta = 0.04145e^{0.06088T} \tag{B2}$$

$$\gamma = \frac{\left(c_p\right)_{air}P}{\lambda_v MW_{ratio}} \tag{B3}$$

$$e_a = 6.112exp\left(\frac{17.67T}{T+243.5}\right) \tag{B4}$$

$$R_n = R_{ns} - R_{nl} \tag{B5}$$

$$R_{ns} = (1-D)R_s \tag{B6}$$

$$R_{nl} = s\left[\frac{T_{max,K}{}^4 + T_{min,K}{}^4}{2}\right]\left(0.34 - 0.14\sqrt{e_d}\right)\left(1.35\frac{R_s}{R_{so}} - 0.35\right) \tag{B7}$$

$$R_s = k_{Rs}\sqrt{T_{max} - T_{min}}R_a \tag{B8}$$

$$R_a = \frac{24\cdot 60}{\pi}G_{sc}d_r\left[\omega_s sin(\phi)sin\left(\delta\right) + cos(\phi)cos\left(\delta\right)sin(\omega_s)\right] \tag{B9}$$

$$R_{so} = \left(0.75 + 2x10^{-5}z_s\right)R_a \tag{B10}$$

$$\phi = \frac{\pi}{180}\left(Lat_{deg} + \frac{Lat_{min}}{60}\right) \tag{B11}$$

$$d_r = 1 + 0.033cos\left(\frac{2\pi J}{365}\right) \tag{B12}$$

$$\delta = 0.409sin\left(\frac{2\pi J}{365} - 1.39\right) \tag{B13}$$

$$\omega_s = acos\left[-tan(\phi)\cdot tan\left(\delta\right)\right] \tag{B14}$$

where,

P : atmospheric pressure (kPa)
λ_v : latent heat of water vaporisation = 2.45 (MJ kg^{-1})
c_p : specific heat of air at constant pressure (MJ kg^{-1} °C^{-1}) = 1012 × 10^{-6}
MW_{ratio}: ratio molecular weight of water vapour/dry air = 0.622
R_{ns} : shortwave net radiation (MJm^{-2}day^{-1})
R_{nl} : long wave net radiation (MJm^{-2}day^{-1})
D : albedo or canopy reflection coefficient = 0.23
s : Stefan-Boltzmann constant = 4.903 × 10-9 (MJK^{4}m^{-2}day^{-1})
$T_{\max}$: maximum absolute temperature during the 24-h period [K = °C + 273.16]
$T_{\min}$: minimum absolute temperature during the 24-h period [K = °C + 273.16]
e_d : actual vapour pressure (kPa)
R_s : solar or short wave radiation (MJK^{4}m^{-2}day^{-1})
R_{so} : clear-sky radiation (MJK^{4}m^{-2}day^{-1})
R_a : extra-terrestrial radiation (MJK^{4}m^{-2}day^{-1})
z_s : station elevation above the sea level
G_{sc} : solar constant = 0.082 (MJm^{-2}min^{-1})
d_r : inverse relative distance Earth-Sun
ω_s : sunset hour angle (rad)
ϕ : latitude (rad)
δ : solar declination (rad)
J : day number within a year i.e. $1 \leq J \leq 365$.

References

Allen, M.R., Smith, M., Pereira, L.S., Perrier, A., 1994. An update for the calculation of reference evapotranspiration. ICID Bull. 43, 35–92.
Baines, G.B.K., 1972. Turbulence within a wheat crop. Agric. Meteorol. 10, 93–105.
Baker, C.J., Berry, P.M., Spink, J.H., Sylvester-Bradley, R., Griffin, J., Scott, R.K., et al., 1998. A method for the assessment of the risk of wheat lodging. J. Theor. Biol. 194, 587–603.
Baker, C.J., Sterling, M., Berry, P., 2014. A generalised model of crop lodging. J. Theor. Biol. 363, 1–12.
Baker, C.J., 1995. The development of a theoretical model for the wind-throw of plants. J. Theor. Biol. 175, 355–372.
Berry, P.M., Sterling, M., Baker, C.J., Spink, J.H., Sparkes, D.L., 2003. A calibrated model of wheat lodging compared with field measurements. Agric. For. Meteorel. 119, 167–180.
Berry, P.M., Sterling, M., Mooney, S.J., 2006. Development of a model of lodging for barley. J. Agron. Crop Sci. 192 (2), 151–158.
Berry, P.M., White, C., Sterling, M., Baker, C., 2013. Develop a model of lodging in oilseed rape to enable integrated lodging control to reduce PGR use. CRD Project PS2146, September.
Cionoco, R.M., 1972. A wind profile index for canopy flow? Boundary Layer Meteorol. 3 (2), 255–263.
Denmead, O., Bradley, E.F., 1967. The Collection and Processing of Field Data. John Wiley and Sons, New York.
Eames, M., Kershaw, T., Coley, D., 2011. On the creation of future probabilistic design weather years from UKCP09. Build. Serv. Eng. Res. Technol. 32 (2), 127–142.
Ekström, M., Jones, P.d., Fowler, H.j., Lenderink, G., Buishand, T.a., Conway, D., 2007. Regional climate model data used within the SWURVE project 1: projected changes in seasonal patterns and estimation of PET. Hydrol. Earth Syst. Sci. 11, 1069–1083.
Finnigan, J.J., Mulheran, P.J., 1978. Modelling waiving crops in a wind tunnel. Boundary Layer Meteorol. 14, 253–277.
Finnigan, J., 2000. Turbulence in plant canopies. Annu. Rev. Fluid Mech. 32, 519–571.
Jenkins, G.J., Murphy, J.M., Sexton, D.M., Lowe, J.A., Kilsby, C.G., 2009. UK Climate Predictions: Briefing Report. Met Office Hadley Centre, Exeter, UK.
Langre, E., 2008. Effect of wind on plants. Annu. Rev. Fluid Mech. 40, 141–168.
Martinez-Vazquez, P., Sterling, M., 2011. Predicting wheat lodging at large scales. Biosyst. Eng. 109 (4), 326–337.
Met Office, 2013. Virtual Met Mast Report for Meteorological Research Unit. Met Office, Cardington.
Rodriguez, M., Moulia, B., De Lagrange, E., 2009. Experimental investigation of a walnut tree multimodal dynamics. In: 7 Euromech Solid Mechanics Conference, Lisbon. 7–11 Sept.
Saunderson, S.E.T., Baker, C.J., England, A., 1999. A dynamical model of the behaviour of Sitka Spruce in high winds. J. Theore. Biol. 2000, 249–259.
Saunderson, S.E.T., Baker, C.J., England, A., 2000. A dynamic analysis of the wind throw of trees? Forestry 73 (3), 225–237.
Sellier, D., Fourcaud, T., Lac, P., 2006. A finite element model for investigating effects of aerial architecture on tree oscillations. Tree Physiol. 26, 799–806.
Sterling, M., Berry, P.M., Baker, C.J., Wade, A., 2003. An experimental investigation of the lodging of wheat. Agric. For. Meteorol. 119, 149–165.
Tsimplis, M.N., 1994. The correlation of wind speed and rain. Weather 49 (4), 135–139.
Ventura, F., Spano, D., Duce, P., Snyder, R.L., 1999. An evaluation of common evapotranspiration equations. Irrig. Sci. 18, 163–170.
Verissimo, H., 2015. Quantification of Cereal Lodging at Small and Large Scales. MSc Thesis. University of Birmingham, UK.
Wright, J.L., 1965. Evaluating Turbulent Transfer Aerodynamically Within the Microclimate of a Cornfield. PhD Thesis. Cornell University, Ithaca, New York.